

# Electrolytic Deposition of Oxide Films in the Presence of Hydrogen Peroxide

I. Zhitomirsky\*

Israel Institute of Metals, Technion-Israel Institute of Technology, Haifa, 32000 Israel

(Received 3 August 1998; accepted 23 January 1999)

## Abstract

*Cathodic electrosynthesis of  $TiO_2$ ,  $Nb_2O_5$ , PZT, composite  $RuO_2$ - $TiO_2$  and  $Al_2O_3$ - $TiO_2$  films and powders was performed. In the proposed approach,  $TiO_2$ ,  $Nb_2O_5$ , PZT film formation on platinized silicon or/and Pt substrates was achieved via peroxoprecursors. Obtained deposits were characterized by XRD, SEM, Auger and SIMS methods. The crystallization behaviour of the deposits has been studied. Possible cathodic reactions which underlie the deposition process and the role of hydrogen peroxide are discussed. © 1999 Published by Elsevier Science Limited. All rights reserved*

**Keywords:**  $Nb_2O_5$ , PZT,  $TiO_2$ ,  $ZrO_2$ ,  $RuO_2$ , electrolytic deposition.

## 1 Introduction

During recent years, interest has been generated in electrolytic deposition of ceramic films.<sup>1–14</sup> This technique can be considered as an important tool in the formation of nanostructured materials, including monolayer and multilayer films, powders and composites.<sup>6,7,10,11,13</sup> Cathodic electrodeposition offers important advantages<sup>2,15</sup> and holds great promise for various applications. A great deal of recent research has been devoted to demonstrating the feasibility of electrodeposition of important ceramic materials.<sup>1–20</sup> Cathodic electrodeposition is achieved via hydrolysis of metal ions or complexes by electrogenerated base to form oxide,<sup>1,6,12,15</sup> hydroxide<sup>3,10,11,16,17</sup> or peroxide<sup>2,7,9,13,18–20</sup> deposits on cathodic substrates. Hydroxide and peroxide deposits can be converted to corresponding oxides by

thermal treatment. Formation of oxide materials via corresponding hydroxides or peroxides constitute two different chemical routes in electrodeposition. In previous work<sup>16</sup> electrodeposition of zirconia was performed via hydroxide and peroxide precursors and obtained results were compared. It should be noted that peroxoprecursor method cannot be applied for deposition of such materials as  $RuO_2$ ,<sup>17,21</sup> as Ru species bring about decomposition of  $H_2O_2$  in solutions. On the other hand peroxoprecursor route was designed in order to solve problems associated with the electrodeposition of  $TiO_2$ ,<sup>2,7,13,21</sup> and  $Nb_2O_5$ .<sup>18</sup> These materials can be deposited via corresponding peroxides. The important finding was that complex oxide compounds such as  $ZrTiO_4$  and PZT can be deposited via peroxoprecursors.<sup>9,13,19,20</sup> It was revealed that the use of the peroxoprecursor approach allows to obtain deposits of desired stoichiometry.  $ZrTiO_4$  and PZT films were obtained after thermal treatment of obtained precursors at relatively low temperatures, in accordance with the temperatures of formation of these materials via the wet chemical method. However, further investigations are necessary to obtain a better understanding of the mechanism of deposition via peroxoprecursors.

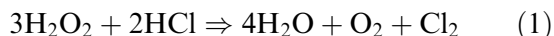
This paper presents results of electrodeposition of ceramic materials in the presence of hydrogen peroxide and addresses different factors controlling deposit composition, morphology and crystallization behaviour.

## 2 Experimental Procedures

As starting materials commercially guaranteed  $TiCl_4$  (Merck),  $NbCl_5$  (Fluka Chemie AG),  $ZrOCl_2 \cdot 8H_2O$  (Fluka Chemie AG),  $RuCl_3 \cdot nH_2O$  (Fluka Chemie AG),  $AlCl_3 \cdot 6H_2O$  (Aldrich Chemical Company, Inc),  $Pb(NO_3)_2$  (Riedel -de Haen) and hydrogen peroxide  $H_2O_2$  (30 wt% in water,

\*Now at: Department of Materials Science and Engineering, McMaster University, 1280 Main Street West, Hamilton, Ontario, Canada L8S 4LZ. Fax: +905 528 9295; e-mail: zhitom@mcmaster.ca/

Carlo Erba) were used. 0.3 M  $\text{TiCl}_4$  solution in methyl alcohol was prepared at  $1^\circ\text{C}$ , then  $\text{H}_2\text{O}_2$  was slowly added ( $\text{H}_2\text{O}_2:\text{TiCl}_4 = 20:1$ ). At this stage significant gas evolution was observed, attributed probably to the following reaction:<sup>22</sup>

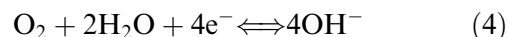
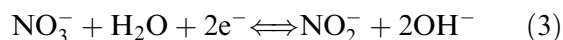
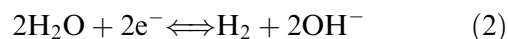


After aging at  $20^\circ\text{C}$  for 3 days this solution was diluted with water and methyl alcohol to obtain stock solution 1 (Table 1). Procedures for preparation of stock solutions 2–9 (Table 1) were similar to those described in previous papers.<sup>18,20,21,23</sup> Electrodeposition was performed at a galvanostatic regime. The electrochemical cell for deposition included the cathodic substrate centered between two parallel platinum counterelectrodes. Pt foils, platinized silicon wafers (Pt/Ti/SiO<sub>2</sub>/Si, 1600 Å Pt, 400 Å Ti, 1000 Å SiO<sub>2</sub>), Ti and graphite plates were used as cathodic substrates. Obtained deposits were washed with water in order to prevent Cl impurity in the solution. Multilayer deposition was performed in order to decrease cracking attributed to drying shrinkage. The microstructure of the obtained deposits was studied using a scanning electron microscope (Jeol, JSM-840) equipped with EDS. X-ray diffraction patterns were obtained using a diffractometer (Phillips, PW-1820,  $\text{CuK}_\alpha$  radiation). For the X-ray studies the deposits were annealed in air at various temperatures. Thin films were also studied by Auger method (scanning microscope Perkin–Elmer, PHI

model 590A) and SIMS method (Cameca IMS 4F ion microscope).

### 3 Results and Discussion

In the cathodic electrodeposition method,<sup>1–3</sup> the following reactions are used to generate base at an electrode surface:



Electrodeposition of  $\text{TiO}_2$  and  $\text{Nb}_2\text{O}_5$  films is achieved via hydrolysis of corresponding peroxocomplexes by electrogenerated base and thermal decomposition of obtained peroxoprecursors.<sup>2,7,13,18</sup> In contrast to Refs. 2,7 and 13 in this work electrodeposition of titania films was performed at  $20^\circ\text{C}$ . Titania films were prepared from stock solution 1 on Pt foils and platinized silicon wafers. Thick deposits (up to  $1\text{--}2\ \mu\text{m}$ ) were obtained by multiple deposition accompanied by drying at  $150^\circ\text{C}$ . As-prepared deposits were found to be amorphous, evidence of crystallinity was observed at temperatures exceeding  $400^\circ\text{C}$ . As can be seen in Fig. 1, peaks of an anatase structure<sup>24</sup> were observed at  $500^\circ\text{C}$ . SIMS analysis revealed residual  $\text{Cl}^-$  in obtained films. SIMS depth profiles of  $\text{Cl}^-$  indicated that the films contained

**Table 1.** Compositions of solutions and experimental conditions of the deposition process

Stock solution	Electrolyte	Solvent	Temperature ( $^\circ\text{C}$ )	Current density ( $\text{mA cm}^{-2}$ )
1	0.005 M $\text{TiCl}_4 + 0.1$ M $\text{H}_2\text{O}_2$	Methyl alcohol– water (3:1 <sup>a</sup> )	20	20
2	0.005 M $\text{NbCl}_5 + 0.05$ M $\text{H}_2\text{O}_2$	Water	1	20
3	$\text{Pb}(\text{NO}_3)_2:\text{ZrOCl}_2:\text{TiCl}_4:\text{H}_2\text{O}_2$ = 1:0.52:0.48:10 $\text{Pb}(\text{NO}_3)_2$ concentration 0.005 M	Water	1	25
4	$\text{TiCl}_4:\text{H}_2\text{O}_2:\text{RuCl}_3 = 1:2:1$ , total concentration of Ti and Ru salts 0.005 M	Methyl alcohol– water (1:1 <sup>a</sup> )	1	20
5	$\text{TiCl}_4:\text{H}_2\text{O}_2:\text{RuCl}_3 = 3:6:1$ , total concentration of Ti and Ru salts 0.005 M	Methyl alcohol– water (3:1 <sup>a</sup> )	1	20
6	$\text{TiCl}_4:\text{H}_2\text{O}_2:\text{RuCl}_3 = 9:18:1$ total concentration of Ti and Ru salts 0.005 M	Methyl alcohol– water (9:1 <sup>a</sup> )	1	20
7	$\text{TiCl}_4:\text{H}_2\text{O}_2:\text{AlCl}_3 = 1:2.5:2$ , total concentration of Ti and Al salts 0.005 M	Methyl alcohol– water (3:1 <sup>a</sup> )	20	20
8	$\text{TiCl}_4:\text{H}_2\text{O}_2:\text{AlCl}_3 = 1:2.5:1$ , total concentration of Ti and Al salts 0.005 M	Methyl alcohol– water (3:1 <sup>a</sup> )	20	20
9	$\text{TiCl}_4:\text{H}_2\text{O}_2:\text{AlCl}_3 = 2:5:1$ , total concentration of Ti and Al salts 0.005 M	Methyl alcohol– water (3:1 <sup>a</sup> )	20	20

<sup>a</sup> Volume ratio.

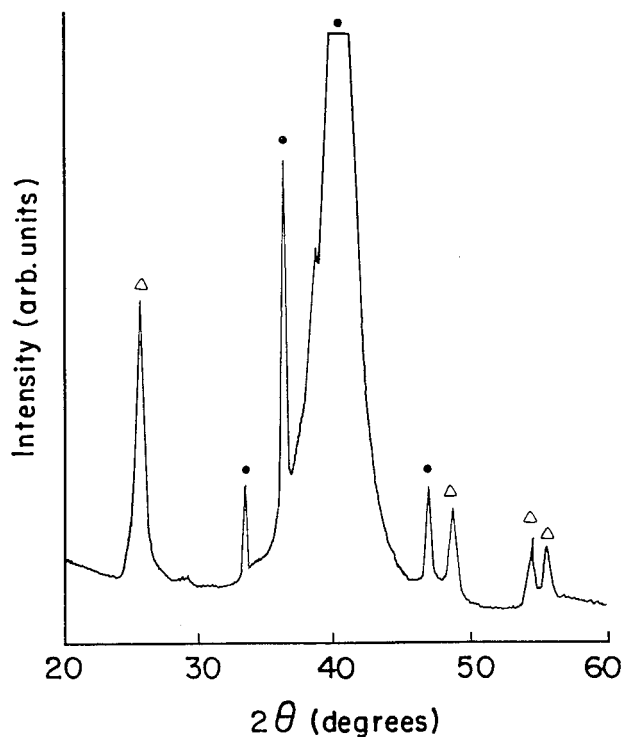


Fig. 1. X-ray diffraction pattern of titania deposit on platinized silicon after thermal treatment at 500°C for 30 min.  $\Delta$ ,  $\text{TiO}_2$  (anatase);  $\bullet$ , substrate.

0.06–0.09 at% of  $\text{Cl}^-$ . At this point it is important to mention that chloride ions can be partially removed from starting solutions through an oxidoreduction<sup>22</sup> process [reaction (1)]. The residual  $\text{Cl}^-$  concentration in the films was comparable with that in chemically precipitated powders obtained in the presence of  $\text{H}_2\text{O}_2$ .<sup>25,26</sup>

Niobium oxide deposits were obtained from stock solution 2. Thick deposits were removed from the Pt substrates for preparation of powder samples. Figure 2 shows X-ray data of the powder samples. The X-ray diffractogram of fresh deposits exhibit their amorphous nature. Crystallization of a pseudo-hexagonal  $\text{Nb}_2\text{O}_5$  phase<sup>27</sup> was observed at 600°C. The results are in agreement with those obtained in previous work.<sup>18</sup> Crystallization of a pseudo-hexagonal  $\text{Nb}_2\text{O}_5$  phase was also observed in  $\text{Nb}_2\text{O}_5$  films and powders prepared by other methods.<sup>28–30</sup> On exposure of obtained deposits to the temperature of 850°C, X-ray diffraction patterns exhibit peaks of orthorhombic form of  $\text{Nb}_2\text{O}_5$ .<sup>31</sup> The formation of orthorhombic  $\text{Nb}_2\text{O}_5$  has been observed in powders obtained by hydrothermal  $\text{H}_2\text{O}_2$  oxidation of Nb<sup>29</sup> and in alkoxide-derived niobium pentoxide gels.<sup>32</sup> After thermal treatment at 1050°C the samples consisted of mixtures of M and H forms of  $\text{Nb}_2\text{O}_5$ .<sup>30,33,34</sup> According to Refs 30 and 33 M- $\text{Nb}_2\text{O}_5$  is considered to be a two-dimensionally ordered H- $\text{Nb}_2\text{O}_5$ . XRD spectra taken from deposits thermally treated at 1200°C show peaks of monoclinic H- $\text{Nb}_2\text{O}_5$ ,<sup>35</sup>

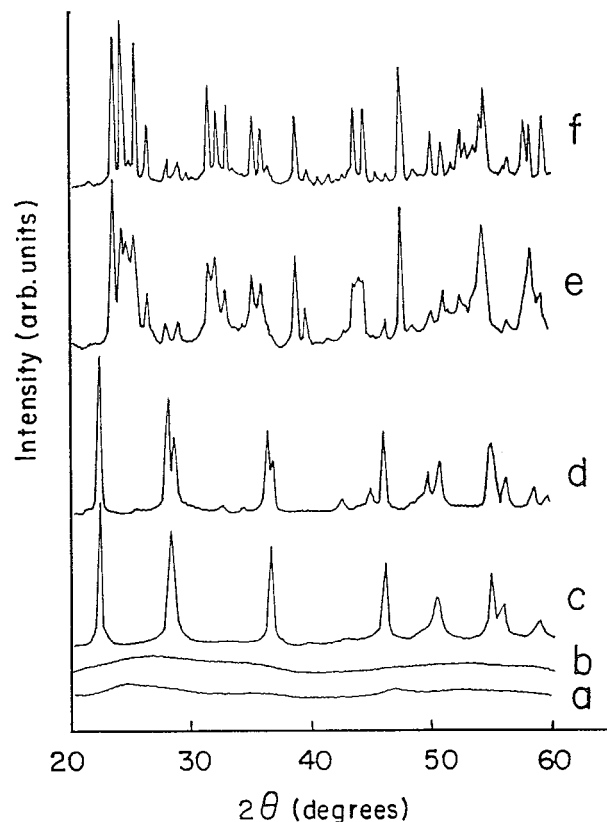


Fig. 2. X-ray diffraction patterns of niobium oxide powders: (a) as prepared, and after thermal treatment at different temperatures for 1 h: (b) 500°C, (c) 600°C, (d) 850°C, (e) 1050°C, (f) 1200°C.

which is the only form stable at room temperature and atmospheric pressure.

Thin  $\text{Nb}_2\text{O}_5$  films (up to 1000 Å) were smooth and adhered well to platinized silicon substrates. Typical Auger depth profile for thin  $\text{Nb}_2\text{O}_5$  film on platinized silicon is shown in Fig. 3. As seen in Fig. 3 at  $\sim 500$  Å, the oxygen peak O and niobium peak Nb begin to decrease; correspondingly the Pt peak begins to increase, signifying the beginning of the

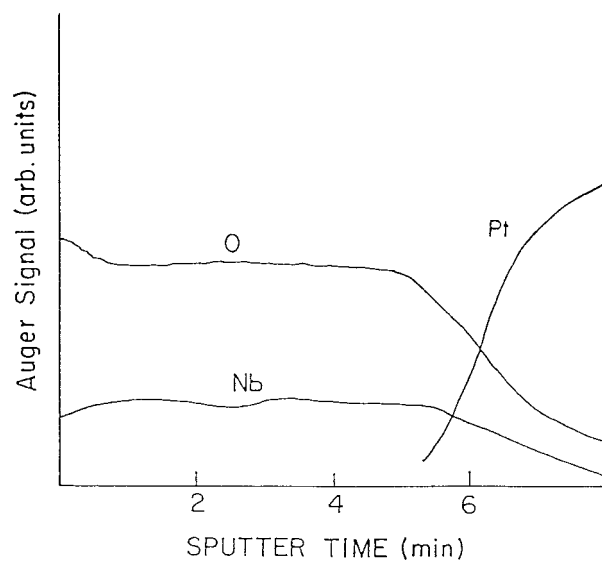


Fig. 3. Auger depth profile of green niobium oxide film on platinized silicon.

transition to platinum. The niobium oxide/platinum surface is not abrupt, but forms a region with a gradient composition. Thick films (1–2  $\mu\text{m}$ ) exhibited microporosity, resulting probably from the gas evolution during electrodeposition (Fig. 4).

Results of this work, coupled with previous results,<sup>2,7,13,18</sup> pave the way for formation of  $\text{TiO}_2$  and  $\text{Nb}_2\text{O}_5$  powders via electrosynthesis and electrodeposition of thin films on various substrates. The possibility of thin film formation on platinized silicon is important for electronic applications. However, further experiments are necessary for optimization of the deposition process in order to prevent microporosity and cracking. Studies in this direction are under way. The peroxoprecursor method developed first for deposition of titania and applied then for deposition of niobium oxide can be used for electrosynthesis of other oxides. Obtained results have practical importance for the development of complex compounds and composite materials. It should be noted that hydrogen peroxide suppresses hydrolysis of titanium and niobium ions,<sup>22,36</sup> which are however able to coprecipitate with other ions.<sup>37–39</sup> Turning to the experiments on powder formation via wet chemical methods it should be mentioned that the use of peroxoprecursors was found to improve coprecipitation and allows different complex oxide compounds of desired stoichiometry to be obtained.<sup>37,40–42</sup> The hydrogen peroxide additive has a number of effects on precipitates, such as conversion of the hydroxide precipitates into hydrated oxides or peroxides, reduction of bridging and non-bridging hydroxogroups in coprecipitates resulting in lower aggregation of dried powders<sup>37,38</sup> and enhancement of crystallization of complex oxides at lower temperatures.<sup>42</sup> According to Ref.25, addition of the  $\text{H}_2\text{O}_2$  inhibits formation of carbonate species when precipitation is performed under a  $\text{CO}_2$  containing atmosphere. Several previous investigations have been undertaken on the

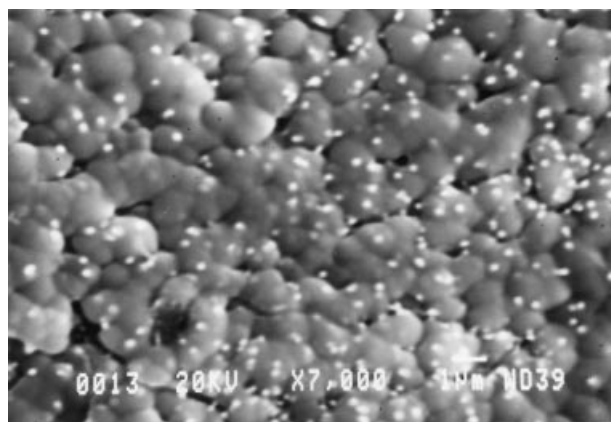


Fig. 4. SEM picture of green niobium oxide film on platinized silicon.

electrosynthesis complex oxide compounds via the peroxoprecursor route including comparison of crystallization behaviour of the complex oxides with the crystallization of individual components. The important finding was that complex oxide compounds such as  $\text{ZrTiO}_4$  and PZT<sup>9,13,19,20</sup> can be deposited via corresponding peroxoprecursors. The experimental results obtained by electrogenerated base method<sup>9,13,19,20</sup> were similar to those obtained by wet chemical methods.<sup>37,38,41,42</sup> As an extension of previous works<sup>9,20</sup> in this work the electrodeposition of PZT was performed on platinized silicon substrates.

Obtained results of X-ray study (Fig. 5) are in a good agreement with previous works.<sup>9,20</sup> As-prepared films were found to be amorphous as indicated by the absence of any well defined diffraction peaks in the XRD patterns apart from peaks of the substrate. The study of phase evolution of obtained films revealed the formation of a perovskite phase at 500°C. Results of X-ray study show that PZT crystallizes directly from the amorphous phase. Typical Auger spectrum of the surface of as-prepared film is shown in Fig. 6. The spectrum revealed Pb, Zr, Ti, O and carbon as a surface contaminant [Fig. 6(a)]. After  $\sim 8000 \text{ \AA}$  sputtering

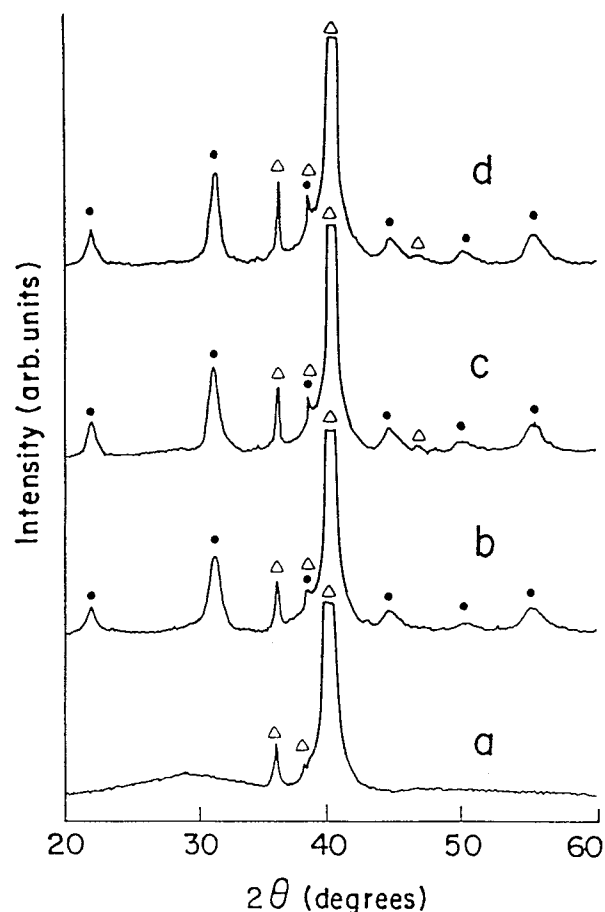


Fig. 5. X-ray diffraction patterns of PZT deposits on platinized silicon substrates: (a) as prepared, and after thermal treatment at different temperatures for 30 min: (b) 500°C, (c) 600°C; (d) 700°C. ●, PZT; Δ, substrate.

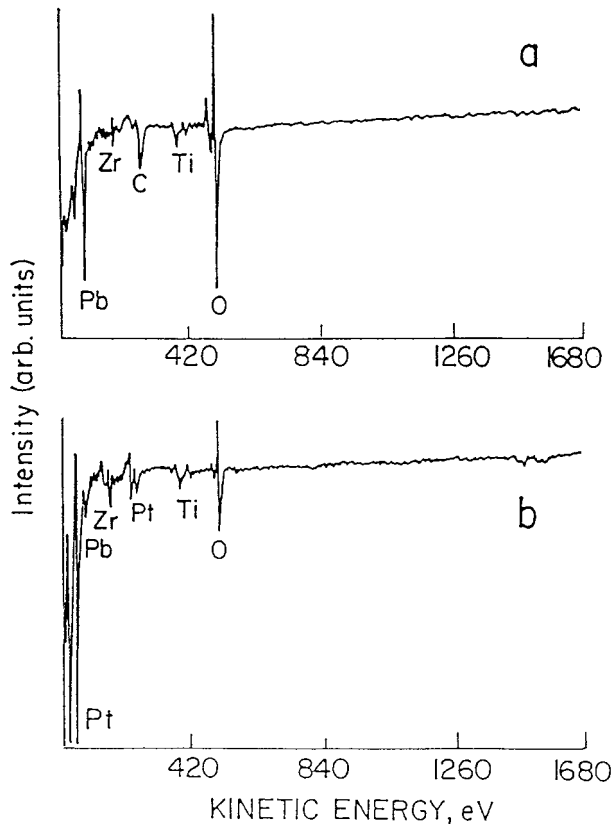


Fig. 6. Auger spectra of (a) the surface and (b) after  $\sim 8000$  Å sputtering of PZT film on platinized silicon.

peaks of Pt were observed in addition to those of Pb, Zr, Ti and O [Fig. 6(b)]. Typical Auger depth profile for PZT film is shown in Fig. 7. Relatively uniform distribution of Ti, Zr and Pb was observed. It should be noted that for important applications of ferroelectric films in different electronic devices the electrodeposition process should be applied to platinized silicon substrates. However, no cathodic deposition of complex titanates on Pt was achieved in other works.<sup>43,44</sup> It is expected that other complex titanates and niobates can be deposited via the peroxoprecursor route.

The feasibility of the deposition of titania films is important for electrodeposition of composite materials. Composite  $\text{RuO}_2\text{-TiO}_2$  and  $\text{Al}_2\text{O}_3\text{-TiO}_2$

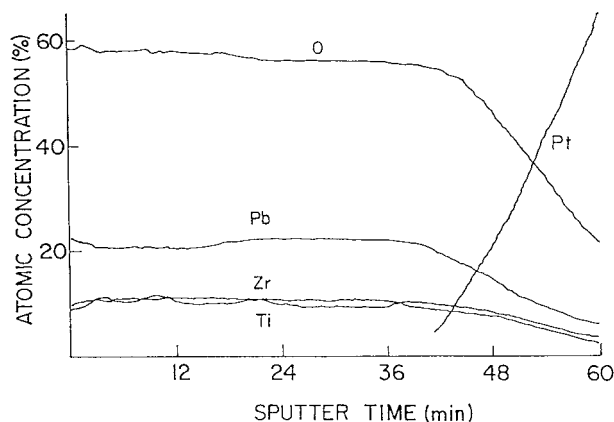


Fig. 7. Auger depth profile of PZT film on platinized silicon.

materials were obtained from stock solutions 4–9. Figure 8 shows EDS spectra for deposits obtained from stock solutions 4–9 (deposits 4–9). Ru/Ti ratio was found to be 0.9, 0.6 and 0.1 for deposits 4, 5 and 6, respectively, obtained on Pt and Ti substrates. The feasibility of cathodic electrodeposition of composite  $\text{RuO}_2\text{-TiO}_2$  films on Ti substrates is important for electrochemical applications.<sup>45–47</sup> Al/Ti ratio was found to be 2.9, 1.3 and 0.6, for deposits 7, 8 and 9, respectively, on graphite substrates. Figure 9 shows SEM pictures of deposits 5 and 6 which were removed from Pt substrates and thermally treated at  $600^\circ\text{C}$  for 1 h. Obtained powder samples contained platelets of uniform thickness in the range of up to  $5\ \mu\text{m}$ .

Cathodic electrodeposition process is based on base generation in electrode reactions and neutralization of ionic species to form deposits. During the deposition process an insulating layer forms, which prevents  $\text{OH}^-$  generation. Coating resistivity is a major limiting factor of the electrodeposition method for development of thick coatings. According to Ref. 1 insulating ceramics form very thin films or porous films. However, it is known that  $\text{RuO}_2$  exhibits metallic resistivity.<sup>48</sup> Therefore, low electric resistivity and higher deposit thickness can be expected for composite materials based on  $\text{RuO}_2$ . Results of this work indicate that thick  $\text{RuO}_2\text{-TiO}_2$  films can be obtained.

As pointed out in Refs. 1–3, the production of  $\text{OH}^-$  increases the local pH, resulting in the precipitation of hydroxides or peroxides. However, according to Ref. 49 the peroxy-based route is completely different from deposition by a local pH increase. It was suggested<sup>49</sup> that in this case a pH increase is detrimental to deposition. At this point it is important to mention that addition of alkali to peroxy-titanate solutions results in precipitation of a peroxo-titanium hydrate.<sup>36</sup> Therefore, the precipitation

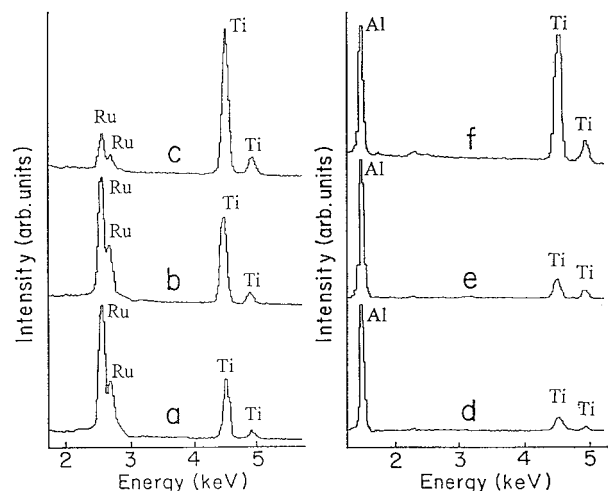


Fig. 8. EDS spectra for deposits obtained from stock solutions (a) 4, (b) 5, (c) 6, (d) 7, (e) 8, (f) 9.

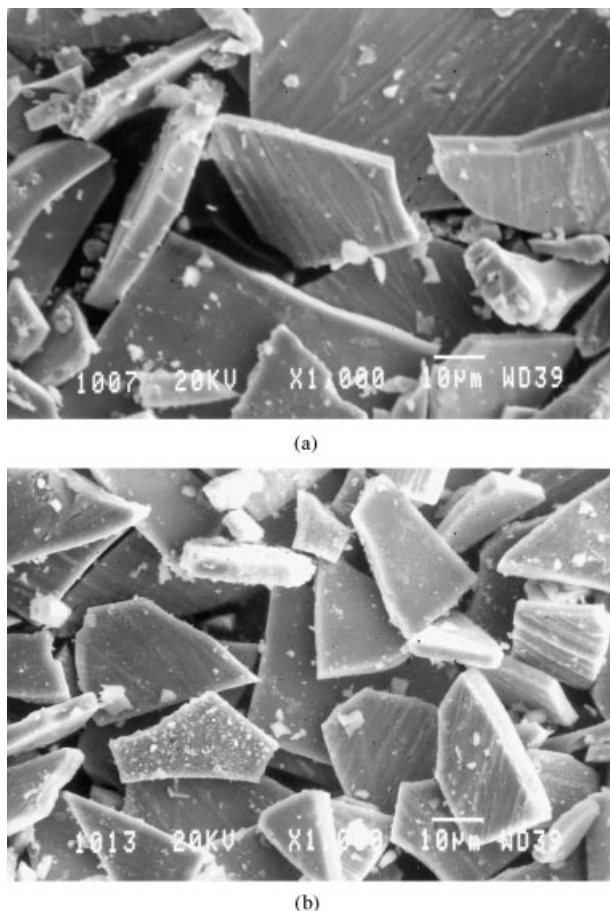


Fig. 9. SEM pictures of deposits (a) 5 and (b) 6 removed from Pt substrates and thermally treated at 600°C for 1 h.

of a peroxotitanium hydrate by electrogenerated base can also be expected.<sup>2</sup> Electrodeposition of titania is achieved via a peroxoprecursor.<sup>2</sup> As pointed out above, the peroxoprecursor method cannot be applied for deposition of RuO<sub>2</sub>, as Ru species bring about decomposition of free H<sub>2</sub>O<sub>2</sub> in solutions. The mechanism underlying the deposition of RuO<sub>2</sub> is based on a local pH increase.<sup>17</sup> Results of this work show that electrodeposition of Ti and electrodeposition of Ru species can be achieved simultaneously. Therefore it may be suggested that both processes are based on a local pH increase.

#### 4 Conclusions

Hydrogen peroxide was utilized to stabilize Ti and Nb species in aqueous solutions and cathodic electro-synthesis of TiO<sub>2</sub> and Nb<sub>2</sub>O<sub>5</sub> films and powders via the corresponding peroxoprecursors has been performed. Crystallization of titania (anatase) was observed at temperatures exceeding 400°C. Metastable pseudohexagonal Nb<sub>2</sub>O<sub>5</sub> phase crystallized at 600°C, on further heating transformation to orthorhombic form (850°C) and monoclinic form (1200°C) was observed. Hydrogen peroxide decreases Cl<sup>-</sup> concentration in solutions, however

the residual Cl<sup>-</sup> concentration in titania films was found to be in the range 0.06–0.09 at%. Electrodeposition of PZT films via the peroxoprecursor method was performed on platinized silicon wafers. The peroxoprecursor method developed for titania electrodeposition was utilized for electrodeposition of composite RuO<sub>2</sub>–TiO<sub>2</sub> and Al<sub>2</sub>O<sub>3</sub>–TiO<sub>2</sub> materials of various compositions. Obtained results pave the way for electrodeposition of other oxides, complex titanates, niobates and composite materials.

#### References

- Switzer, J. A., Electrochemical synthesis of ceramic films and powders. *Am. Ceram. Soc. Bull.*, 1987, **66**, 1521–1524.
- Zhitomirsky, I., Gal-Or, L., Kohn, A. and Henniecke, H. W., Electrodeposition of ceramic films from non-aqueous and mixed solutions. *J. Mat. Sci.*, 1995, **30**, 5307–5312.
- Gal-Or, L., Silberman, I. and Chaim, R., Electrolytic ZrO<sub>2</sub> coatings I. Electrochemical aspects. *J. Electrochem. Soc.*, 1991, **138**, 1939–1942.
- Aries, L., Roy, J., Sotoul, J., Pontet, V., Costeseque, P. and Aigouy, T., Electrochemically induced alumina coatings on stainless steel: composition and behaviour at high temperature. *J. Appl. Electrochem.*, 1996, **26**, 617–622.
- Aries, L., Preparation of electrolytic ceramic films on stainless steel conversion coatings. *J. Applied Electrochem.*, 1994, **24**, 554–558.
- Zhou, Y., Phillips, R. J and Switzer, J. A., Electrochemical synthesis and sintering of nanocrystalline cerium (IV) oxide powders. *J. Am. Ceram. Soc.*, 1995, **78**, 981–985.
- Zhitomirsky, I., Cathodic electro-synthesis of titania films and powders. *NanoStruct. Mater.*, 1997, **8**, 521–528.
- Abolmaali, S. B. and Talbot, J. B., Synthesis of superconductive thin films of YBa<sub>2</sub>Cu<sub>3</sub>O<sub>7-x</sub> by a nonaqueous electrodeposition process. *J. Electrochem. Soc.*, 1993, **140**, 443–445.
- Zhitomirsky, I., Gal-Or, L., Kohn, A. and Spang, M. D., Electrolytic PZT films. *J. Mat. Sci.*, 1997, **32**, 803–807.
- Zhitomirsky, I., Chaim, R., Gal-Or, L. and Bestgen, H., Electrochemical Al<sub>2</sub>O<sub>3</sub>–Cr<sub>2</sub>O<sub>3</sub> alloy coatings on non-oxide ceramic substrates. *J. Mat. Sci.*, 1997, **32**, 5205–5213.
- Chaim, R., Zhitomirsky, I., Gal-Or, L. and Bestgen, H., Electrochemical Al<sub>2</sub>O<sub>3</sub>–ZrO<sub>2</sub> composite coatings on non-oxide ceramic substrates. *J. Mat. Sci.*, 1997, **32**, 389–400.
- Peulon, S. and Lincot, D., Cathodic electrodeposition from aqueous solution of dense or open-structured zinc oxide films. *Advanced Materials*, 1996, **8**, 166–170.
- Zhitomirsky, I. and Gal-Or, L., Cathodic electro-synthesis of ceramic deposits. *J. Eur. Ceram. Soc.*, 1996, **16**, 819–824.
- Zhitomirsky, I., Electrophoretic and electrolytic deposition of ceramic coatings on carbon fibers. *J. Eur. Ceram. Soc.*, 1998, **18**, 849–856.
- Zhitomirsky, I., Gal-Or, L., Kohn, A. and Henniecke, H. W., Electrochemical preparation of PbO films. *J. Mat. Sci., Lett.*, 1995, **14**, 807–810.
- Zhitomirsky, I. and Gal-Or, L., Characterization of zirconium, lanthanum and lead oxide deposits prepared by cathodic electro-synthesis. *J. Mat. Sci.*, 1998, **33**, 699–705.
- Zhitomirsky, I. and Gal-Or, L., Ruthenium oxide deposits prepared by cathodic electro-synthesis. *Mater. Lett.*, 1997, **31**, 155–159.
- Zhitomirsky, I., Electrolytic deposition of niobium oxide films. *Mater. Lett.*, 1998, **35**, 188–193.

19. Zhitomirsky, I., Gal-Or, L. and Klein, S., Electrolytic deposition of ZrTiO<sub>4</sub> films. *J. Mat. Sci., Lett.*, 1995, **14**, 60–62.
20. Zhitomirsky, I., Kohn, A. and Gal-Or, L., Cathodic electrosynthesis of PZT films. *Mater. Lett.*, 1995, **25**, 223–227.
21. Zhitomirsky, I., Cathodic electrosynthesis of titanium and ruthenium oxides. *Mater. Lett.*, 1998, **33**, 305–310.
22. Alquier, C., Vandenborre, M. T. and Henry, M., Synthesis of niobium pentoxide gels. *J. Non-Cryst. Solids*, 1986, **79**, 383–395.
23. Zhitomirsky, I. and Gal-Or, L., Electrochemical coatings. In *High Temperature Coatings*, ed. N. B. Dahotre. Marcel Dekker, New York, 1999, pp. 83–145.
24. Joint Committee on Powder Diffraction Standards, Powder Diffraction File 21-1272, Swarthmore, PA, 1980.
25. Fox, G. R., Adair, J. H. and Newnham, R. E., Effect of pH and H<sub>2</sub>O<sub>2</sub> upon coprecipitated PbTiO<sub>3</sub> powders: Part I. Properties of as-precipitated powders. *J. Mat. Sci.*, 1990, **25**, 3634–3640.
26. Fox, G. R., Breval, E. and Newnham, R. E., Crystallization of nanometre-size coprecipitated PbTiO<sub>3</sub> powders. *J. Mat. Sci.*, 1991, **26**, 2566–2572.
27. Joint Committee on Powder Diffraction Standards, Powder Diffraction File 28-317, Swarthmore, PA, 1986.
28. Ohtani, B., Iwai, K., Nishimoto, S. and Inui, T., Electrochromism of niobium oxide thin films prepared by the sol-gel process. *J. Electrochem. Soc.*, 1994, **141**, 2439–2442.
29. Wang, C., Su, Q., Liu, F., Qian, Y. and Zhao, G., Preparation of ultrafine powders of N<sub>2</sub>O<sub>5</sub> by hydrothermal H<sub>2</sub>O<sub>2</sub> oxidation starting from metallic Nb. *NanoStruct. Mater.*, 1997, **8**, 163–169.
30. Narendar, Y. and Messing, G. L., Synthesis, decomposition and crystallization characteristics of peroxo-citratoniobium: an aqueous niobium precursor. *Chem. Mater.*, 1997, **9**, 580–587.
31. Joint Committee on Powder Diffraction Standards, Powder Diffraction File 27-1003, Swarthmore, PA, 1986.
32. Bansal, N. P., Synthesis and thermal evolution of structure in alkoxide-derived niobium pentoxide gels. *J. Mat. Sci.*, 1994, **29**, 4481–4486.
33. Holtzberg, F., Reisman, A., Berry, M. and Berkenblit, M., Chemistry of the group VB pentoxides. VI. The polymorphism of Nb<sub>2</sub>O<sub>5</sub>. *J. Am. Chem. Soc.*, 1957, **79**, 2039–2043.
34. Schäfer, F., Gruehn, R. and Schulte, F., Die Modifikationen des Niobpentoxids. *Angew. Chem.*, 1966, **78**, 28–41.
35. Joint Committee on Powder Diffraction Standards, Powder Diffraction File 37-1468, Swarthmore, PA, 1987.
36. Mühlebach, J., Müller, K. and Schwarzenbach, G., The peroxo complexes of titanium. *Inorg. Chem.*, 1970, **9**, 2381–2390.
37. Murata, M., Wakino, K., Tanaka, K. and Hamakawa, Y., Chemical preparation of PLZT powder from aqueous solution. *Mat. Res. Bull.*, 1976, **11**, 323–328.
38. Yoshikawa, Y. and Tsuzuki, K., Susceptibility to agglomeration of fine PLZT powders prepared from nitrate solutions. *J. Eur. Ceram. Soc.*, 1990, **6**, 227–235.
39. Yoshikawa, Y. and Uchino, K., Chemical preparation of lead containing niobate powders. *J. Am. Ceram. Soc.*, 1996, **79**, 2417–2421.
40. Gherardi, P. and Matijevic, E., Homogeneous precipitation of spherical colloidal barium titanate particles. *Colloids and Surfaces*, 1988, **32**, 257–274.
41. Navio, J. A., Marchena, F. J., Macias, M., Sanchez-Soto, P. J. and Pichat, P., Formation of zirconium titanate powder from a sol-gel prepared reactive precursor. *J. Mat. Sci.*, 1992, **27**, 2463–2467.
42. Navio, J. A., Macias, M. and Sanchez-Soto, P. J., On the influence of chemical processing in the crystallization behaviour of zirconium titanate materials. *J. Mat. Sci. Lett.*, 1992, **11**, 1570–1572.
43. Matsumoto, Y., Morikawa, T., Adachi, H. and Hombo, J., A new preparation method of barium titanate perovskite film using electrochemical reduction. *Mater. Res. Bull.*, 1992, **27**, 1319–1327.
44. Matsumoto, Y., Adachi, H. and Hombo, J., New preparation method for PZT films using electrochemical reduction. *J. Am. Ceram. Soc.*, 1993, **76**, 769–772.
45. Czarnetzki, L. R. and Janssen, L. J. J., Formation of hypochlorite, chlorate and oxygen during NaCl electrolysis from alkaline solutions at an RuO<sub>2</sub>/TiO<sub>2</sub> anode. *J. Appl. Electrochemistry*, 1992, **22**, 315–324.
46. Bandi, A. and Kühne, H. M., Electrochemical reduction of carbon dioxide in water: analysis of reaction mechanism on ruthenium–titanium–oxide. *J. Electrochem. Soc.*, 1992, **139**, 1605–1610.
47. Hine, F., Yasuda, M. and Yoshida, T., Studies on the oxide-coated metal anodes for chlor-alkali cells. *J. Electrochem. Soc.*, 1977, **124**, 500–505.
48. Ryden, W. D., Lawson, A. W. and Sartain, C. C., Electrical transport properties of IrO<sub>2</sub> and RuO<sub>2</sub>. *Physical Review B*, 1970, **1**, 1494–1500.
49. Meulenkamp, E. A., Mechanism of WO<sub>3</sub> electrodeposition from peroxy–tungstate solution. *J. Electrochem. Soc.*, 1997, **144**, 1664–1671.